Ryanodine receptor dysfunction causes senescence and fibrosis in Duchenne dilated cardiomyopathy

Monia Souidi, Jessica Resta, Haikel Dridi, Yvonne Sleiman, Steve Reiken, Karina Formoso, Sarah Colombani, Pascal Amédro, Pierre Meyer, Azzouz Charrabi, et al.

Ryanodine receptor dysfunction causes senescence and fibrosis in Duchenne dilated cardiomyopathy

Monia Souidi [1], Jessica Resta [2], Haikel Dridi [3], Yvonne Sleiman [1], Steve Reiken [3], Karina Formoso [2], Sarah Colombani [1], Pascal Amédro [1 4], Pierre Meyer [1 5], Azzouz Charrabi [1], Marie Vincenti [1 4], Yang Liu [3], Rajesh Kumar Soni [6], Frank Lezoualc'h [2], D V M Stéphane Blot [7], François Rivier [1 5], Olivier Cazorla [1], Angelo Parini [2], Andrew R Marks [3], Jeanne Mialet-Perez [2 8], Alain Lacampagne [1], Albano C Meli [1]

[1] PhyMedExp, University of Montpellier, INSERM, CNRS, Montpellier, France.

[2] Institute of Metabolic and Cardiovascular Diseases (I2MC), INSERM, University of Toulouse, Toulouse, France.

[3] Department of Physiology and Cellular Biophysics, Clyde and Helen Wu Center for Molecular Cardiology, Columbia University Vagelos College of Physicians and Surgeons, New York, NY, USA.

[4] Department of Pediatric and Congenital Cardiology, M3C Regional Reference CHD Centre, Clinical Investigation Centre, Montpellier University Hospital, Montpellier, France.

[5] Department of Pediatric Neurology, Reference Center for Neuromuscular Diseases AOC, Clinical Investigation Centre, Montpellier University Hospital, Montpellier, France.

[6] Proteomics and Macromolecular Crystallography Shared Resource, Herbert Irving Comprehensive Cancer Center, New York, NY, USA.

[7] IMRB - Biology of the neuromuscular system, INSERM, UPEC, EFS, EnvA, Maisons-Alfort, France.

[8] MitoLab Team, UMR CNRS 6015, INSERM U1083, MitoVasc Institute, Angers University, Angers, France.

Keywords:

Calcium; DMD; Ryanodine receptor; Senescence; hiPSC-derived cardiomyocytes.

Abstract

Background:

Duchenne muscular dystrophy (DMD) is an X-linked disorder characterized by progressive muscle weakness due to the absence of functional dystrophin. DMD patients also develop dilated cardiomyopathy (DCM). We have previously shown that DMD (mdx) mice and a canine DMD model (GRMD) exhibit abnormal intracellular calcium (Ca^{2+}) cycling related to early-stage pathological remodelling of the ryanodine receptor intracellular calcium release channel (RyR2) on the sarcoplasmic reticulum (SR) contributing to age-dependent DCM.

Methods:

Here, we used hiPSC-CMs from DMD patients selected by Speckle-tracking echocardiography and canine DMD cardiac biopsies to assess key early-stage Duchenne DCM features.

Results:

Dystrophin deficiency was associated with RyR2 remodelling and SR Ca^{2+} leak (RyR2 Po of 0.03 ± 0.01 for HC vs. 0.16 ± 0.01 for DMD, $P < 0.01$), which led to early-stage defects including senescence. We observed higher levels of senescence markers including p15 (2.03 ± 0.75 for HC vs. 13.67 ± 5.49 for DMD, $P < 0.05$) and p16 (1.86 ± 0.83 for HC vs. 10.71 ± 3.00 for DMD, $P < 0.01$) in DMD hiPSC-CMs and in the canine DMD model. The fibrosis was increased in DMD hiPSC-CMs. We observed cardiac hypocontractility in DMD hiPSC-CMs. Stabilizing RyR2 pharmacologically by S107 prevented most of these pathological features, including the rescue of the contraction amplitude (1.65 ± 0.06 μm for DMD vs. 2.26 ± 0.08 μm for DMD + S107, $P < 0.01$). These data were confirmed by proteomic analyses, in particular ECM remodelling and fibrosis.

Conclusions:

We identified key cellular damages that are established earlier than cardiac clinical pathology in DMD patients, with major perturbation of the cardiac ECC. Our results demonstrated that cardiac fibrosis and premature senescence are induced by RyR2 mediated SR Ca^{2+} leak in DMD cardiomyocytes. We revealed that RyR2 is an early biomarker of DMD-associated cardiac damages in DMD patients. The progressive and later DCM onset could be linked with the RyR2-mediated increased fibrosis and premature senescence, eventually causing cell death and further cardiac fibrosis in a vicious cycle leading to further hypocontractility as a major feature of DCM. The present study provides a novel understanding of the pathophysiological mechanisms of the DMD-induced DCM. By targeting RyR2 channels, it provides a potential pharmacological treatment.

Background

Duchenne muscular dystrophy (DMD) is an X-linked degenerative disorder with a prevalence of 1/3600–6000 in males due to the absence of functional dystrophin in muscles. DMD causes muscle weakness, respiratory failure and cardiac complications. DMD patients can present with arrhythmias, dilated cardiomyopathy (DCM) progressing to heart failure and sudden death.1DMD-associated cardiac disorders, mainly DCM, reduce life expectancy of patients.2Amedroet al. showed that conventional echocardiography fails to detect early signs of cardiac alterations, whereas Speckle-tracking echocardiography (STE) serves as a functional biomarker to identify early-stage left ventricle motion abnormalities.

The cellular pathophysiological mechanisms underlying the early cardiac damages in DMD remain poorly under-stood. Several studies have focused on defects in cardiac excitation-contraction coupling (ECC) that appears stronglyaltered.3Moreover, functional changes in intracellular Ca2+homeostasis in Duchenne DCM have been linked to post-translational changes in Ca2+signalling proteins. The RyR2macromolecular complex undergoes post-translational modifications and leak, which leads to cardiac dysfunction in the DMD mouse model (mdx)4and GRMD.5We have shown that DMD patient-specific hiPSC-derived cardiomyocytes (hiPSC-CMs) exhibit abnormal ECC.3Thesefindings show that sarco-plasmic reticulum (SR) Ca2+leak largely contributes to the pathogenesis of DMD-associated cardiac dysfunction in mouse, dog and humans.

Here, we selected three DMD boys using STE and studied their hiPSC-CMs to investigate the early-stage properties of the cardiac ECC and cardiac morphology in DMD by focusing on the intracellular Ca2+cycling in connection with markers of fibrosis and senescence. We also exploited canine DMD (GRMD) cardiac biopsies to assess the cardiac senescence. We found that premature senescence and cardiac fibrosis are induced by SR Ca2+leak via RyR2 in DMD cardiomyocytes. Stabilizing RyR2 prevented most of these pathological features. The present study provides new pathophysiological mechanisms and potential pharmacological treatment of the DMD-induced DCM.

Methods

Ethics statement

Written informed consent was obtained from all participating patients for obtaining blood samples for hiPSC generation. The study adhered to the principles of the Declaration of Helsinki and was approved by the Institutional Review Board

Committee of the Montpellier Hospital (2017-A01589-44).Clinical data of the three DMD patients are provided in Table S1. The three male healthy control hiPSC lines used in this study were previously characterized.6–8

Echocardiographic follow-up

Echocardiographic examinations were performed using the GE Vivid E9 ultrasound system. LV function variables, including LV ejection fraction (LVEF) measured using the Teischolz method (M-mode), were collected. Speckle tracking echocardiography was conducted offline by a single senior paediatric cardiologist with expertise in 2D-strain analysis, utilizing

EchoPAC version 112 (GE Healthcare). The endocardium was manually traced in end-diastole, and the software automatically detected myocardial wall movement from endocardium to epicardium, defining areas of interest. Global and segmental LV peak systolic strain variables were measured based on the 17-segment model.

hiPSC generation and maintenance

We generated hiPSC lines from three different DMD boys (9,12 and 14 years old, respectively) as previously described.7Three HC hiPSC lines were used in this work as publishedbefore.9

Cardiac differentiation

hiPSC were differentiated into cardiomyocytes using the 2D-sandwich monolayer protocol as previously described.8–10Allexperiments used hiPSC-CMs aged 30 days and were performed in at least three independent cardiac differentiations.

RT-PCR and qRT-PCR

RT-PCR and qRT-PCR experiments were performed as previously published.9RPLPO and RPL32 were respectively used as reference genes. Primers for human and canine markers expression are listed in Tables S2 and S3.

Immunocytochemistry

Immunocytochemistry experiments were performed on 30-day-old hiPSC-CMs. The cells were fixed with 4% paraformaldehyde and sucrose for 20 min at 37°C and then permeabilized and blocked with 1% BSA and 0.1% Triton 100× for30 min at room temperature. Primary antibodies (Table S4) were applied at 1:200 dilution in 1% BSA and incubated over-night at 4°C. After three washes with PBS, DAPI and secondary antibodies (1:250) were applied for 1 h at room temperature. The coverslips were mounted with Prolong Gold Antifade Mountant. Image acquisition was performed using an inverted confocal microscope (Zeiss LSM 800 with Zen software). Pixel intensity and cell/nuclei area were calculated using ImageJ software.

Measurement of contractile properties

Contractile properties were measured using Zeiss Observer 7microscope equipped with a camera and a thermostatic chamber as we published before.6,9The hiPSC-CMs were incubated over-night with S107 (5μM) prior video-edge experiments acquisition.

Measurement of cytosolic Ca2+variations

Cytosolic Ca2+variations or Ca2+transients were measured as previously published.9S107 (5μM) was tested: hiPSC-CMs were incubated overnight with S107 prior Ca2+variation measurements.

Sarcoplasmic reticulum vesicle preparation

SR vesicles were isolated from hiPSC-CMs as previously published.11S107 treatment (5μM) was performed over-night on DMD hiPSC-CMs prior SR vesicle preparation.

Measurement of RyR2single channel activity

SR vesicles containing RyR2 were fused to planar lipid bilayers formed by painting a lipid solution of as olectin (type IV, Sigma) at 45 mg/mL in decane at RT as previouslydescribed.12–14The channel properties including Po and Fo were determined as previously described.14

Immunoprecipitation, western blots and immunoblot analysis

RyR2 co-immunoprecipitation was performed as previously.9

Senescence-associated beta-galactosidase (SA-β-gal) staining

SA-β-gal staining was performed on 30-day-old HC and DMD hiPSC-CMs following the manufacturer's protocol (Cell Signal-ling, cat#9860). The hiPSC-CMs were coated on Lab-TeK II Chambered #1.5 German Cover glass System (From Nunc, cat#155382) and washed with PBS 1×. For S107 treatment, DMD hiPSC-CMs were treated with 5μM S107 for 10 days. Cardiomyocytes were fixed for 15 min, followed by incubation withβ-galactosidase staining solution at 37°C for approximately 36 h in a humidified chamber. After washing with PBS1×, hiPSC-CMs were incubated with haematoxylin for 2 min, washed again, and mounted with Prolong Gold Antifade Mountant (Thermo Fisher, cat#P36930). Images were taken using a bright field microscope.

GRMD cardiac biopsies

Cardiac tissue was obtained from Golden Retriever Muscular Dystrophy (GRMD, n= 8) canine model at 6 to 12 months of age (Mézilles, France) and age matched normal healthy golden retriever dogs of the same genetic background(n= 6) as previously published.15

Luminex immunoassay

A Luminex™ System was used to measure the cytokine secretion levels of HC and DMD supernatant samples using Milliplex Human Cytokine/Chemokine/Growth Factor Panel A kit (Millipore, cat#HCYTA-60 K) according to manufacturers' protocols. The cytokines included IL-α, IL-1ß, IL-6, IL-18, IFNγand TNFα.

Global quantitative proteomic analysis

Global quantitative proteomics was performed as previouslypublished.16The protein–protein interaction (PPI) networks were constructed using STRING online tool (https://string-db.org/). Volcano plots were used to represent the comparisons HC versus DMD and DMD versus DMD + S107. Gene ontology (GO) analysis was performed using online tool Metascape (http://metascape.org) and the most representative pathways were graphed using Prism.

Statistical analysis

Normality was verified using the D'Agostino & Pearson omnibus normality test. An unpaired t-test compared two independent groups with parametric distribution, while a Mann–Whitney test assessed non-parametric distributions. A two-way ANOVA compared more than two groups ± treatment with normal distribution, and a Kruskal–Wallis test was used for non-parametric distributions. Data are expressed as mean ± SEM, and significance was set at $P<0.05$ (*$P<0.05$;**$P<0.01$). Prism software performed data analysis and statistics.

Results

Echocardiographic assessment of three DMD patients

We followed up the three DMD children using echocardiography by measuring the left ventricular ejection fraction (LVEF) and by speckle tracking echocardiography (STE). Blood samples from the three DMD children were taken at 8, 12 and13 years old, respectively. We reported normal-ranged standard echo parameters (LVEF) for all three DMD children over-time and at 2 time points (Figure S1A, B). Regarding the LV global longitudinal strain (GLS), DMD 1 and 2 exhibited normal-ranged and were stable over their follow-up period (6 and 13 years old and 10 and 13 years old, respectively).DMD 3 showed a lower initial GLS result, which decreased over time (Figure S1C, D). We observed an LV segmental longitudinal strain decrease in inferolateral and anterolateral segments in the basal area for all three DMD, with worsened impairment in DMD 3 at 6 and 13 years old (Figure S1C, D).

DMD hiPSC-CMs lack full length dystrophin isoform

To verify that DMD hiPSC-CMs lack the full-length dystrophin that is the active form in muscles, we performed immuno-blotting and immunocytochemistry experiments to stain respectively the N-and C-terminal domains of full-length dystrophin isoform (427 kDa). As shown in Figure S2A, the three DMD hiPSC-CMs (DMD 1, 2 and 3, harbouring exon 1, 52and 55 deletions, respectively) do not express the full-length dystrophin isoform contrary to the three HC hiPSC-CMs. Immunocytochemistry staining confirmed the absence of the C-terminal and N-terminal domains in DMD hiPSC-CMs (Figure S2B). The clinical data of the selected DMD patients are summarized in Table S1.

S107prevents RyR2leak and post-translational modifications in the three DMD patient hiPSC-CMs

Based on previous work, including ours,4,17 we first hypothesized that RyR2 channels cause diastolic Ca2+leak as such evidence was never proved in DMD patients. To test this hypothesis, we performed bilayer experiments for RyR2 single channel recordings from three

HC and three DMD patient hiPSC-CMs. To discriminate any difference between patientRyR2 channel properties, we coloured each HC and DMDRyR2 channel values. Representative recordings showed ab-errant RyR2 single channels behaviour in DMD hiPSC-CMs (Figure1A). At a Ca2+concentration of 150 nM in the cis-chamber (diastolic condition), we observed an increase in the single channel open probability (Po) in DMD hiPSC-CMs compared with HC hiPSC-CMs (Figure1B). The increased RyR2 Po in DMD hiPSC-CMs was accompanied by increased frequency of opening (Figure1C). We observed no difference in Po between the three HC and three DMD RyR2 channel populations (Figure1B).

We and other have shown that S107 specifically stabilizes the closed conformation of RyR2 without any off-target.4,9We tested S107 in DMD hiPSC-CMs. S107 prevented RyR2 diastolic leak as evidenced by significantly decreasing Po(Figure1B) and Fo(Figure1C). The change in Po was comparable between each patient (Figure1D).

We evaluated the effect of the three dystrophin mutations on the RyR2 expression and its stabilizing partner Calstabin2.HC and DMD hiPSC-CMs express both proteins at 30 days of age (Figure S3A). We observed no difference in the total protein expression for these two proteins in HC and DMD hiPSC-CMs (Figure S3B, C).

We performed RyR2 co-immunoprecipitation experiments to evaluate the RyR2 macromolecular complex remodelling. We assessed the RyR2 PKA and CaMKII phosphorylation level, oxidation, cysteine S-nitrosylation and the amount ofcalstabin2 bound to the channel in HC and DMD hiPSC-CMs.

At rest, we observed higher PKA phosphorylation(Figure S4A,B), cysteine S-nitrosylation (Figure S4A,C) and oxidation (Figure S4A,E) levels in DMD hiPSC-CMs compared with HC hiPSC-CMs. DMD hiPSC-CMs were also significantly more depleted in calstabin2 than HC hiPSC-CMs(Figure S4A–F). No significant difference was observed on CaMKII phosphorylation level between HC hiPSC-CMs and DMD hiPSC-CMs (Figure S4A–D). Under stress, S107 was able to prevent the calstabin2 depletion in DMD hiPSC-CMs (Figure1E,F). PKA-phosphorylation (Figures1E and S5A),CaMKII-phosphorylation (Figures1Eand S5B),S-nitrosylation (Figure1E and S5C) and oxidation (Figures1Eand S5D) levels remain unchanged between HC hiPSC-CMs and DMD hiPSC-CMs, and unaffected by S107.

SR Ca2+leak leads to signalling pathways involving fibrosis and senescence in DMD hiPSC-CMs

To further investigate the consequences of RyR2 dysfunction, we performed proteomic analyses. Hierarchical clustering of the differentially expressed proteins (DEPs) showed that the three HC populations exhibit similar protein expression clusters when compared with the three DMD populations. S107treatment was able to change the DMD profile to HC-like profile (Figures2A, B and S6A, B). We observed that significant biological processes were dysregulated in DMD and prevented by S107, in particular the external encapsulating structure organization, extracellular matrix and structure organizations and glycoprotein

metabolic process (Figure2C). Among the latter, we observed the modified pathways related to extra-cellular matrix in DMD hiPSC-CMs that are prevented by S107.

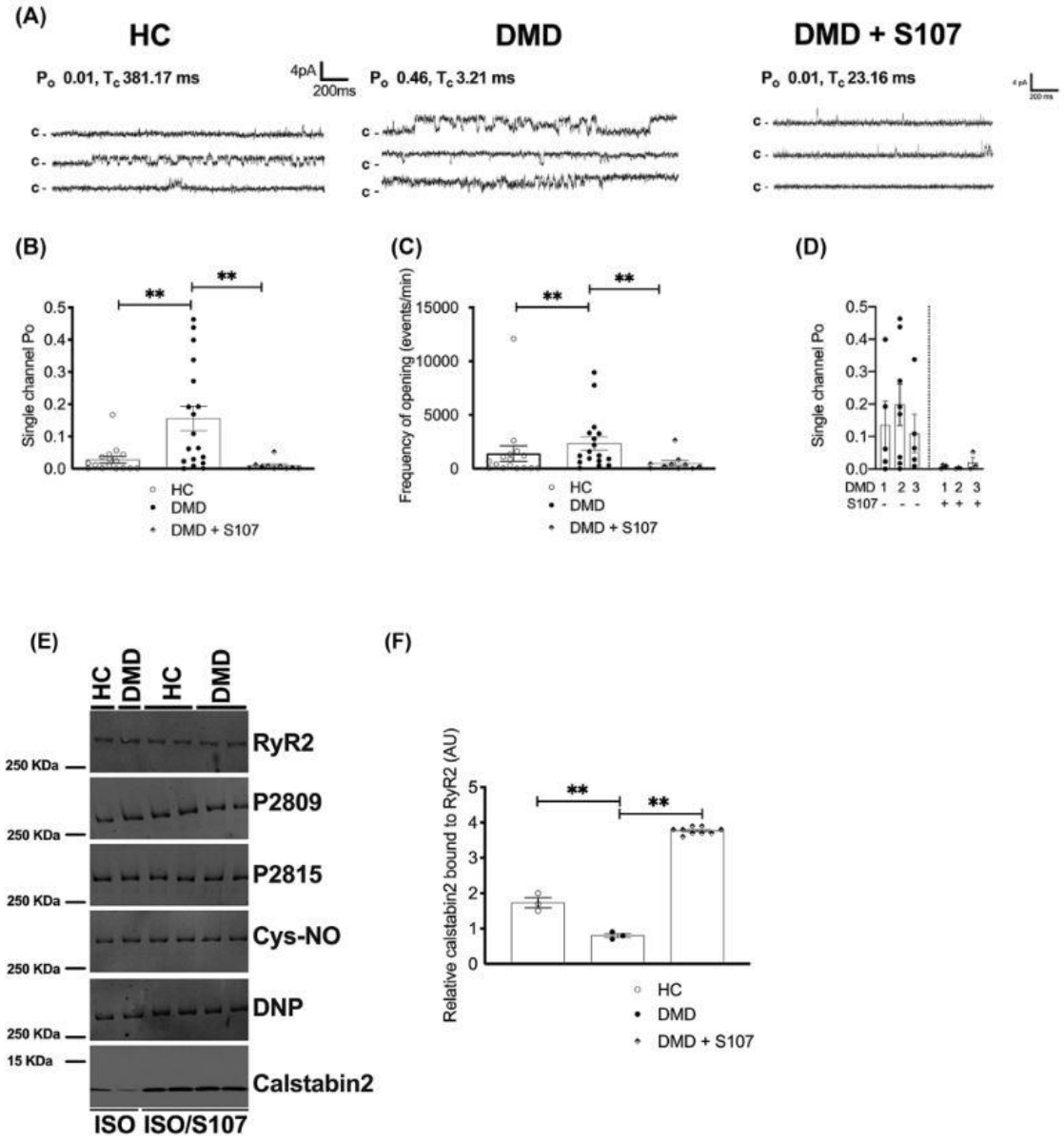

Figure 1 S107 prevents the stress-induced RyR2 Ca^{2+} leak and post-translational remodelling in the three DMD patient hiPSC-CMs. (A) Representative illustrations of RyR2 single channel recordings under 150 nmol/L free *cis* [Ca^{2+}] in HC, DMD hiPSC-CMs. DMD hiPSC-CMs treated with S107 (5 μM overnight). The « c- » represents the RyR2 channel closed state. (B) Bar chart with each data point superimposed showing the single channel open probability (Po) of RyR2 channels in healthy control (HC) and DMD ± S107 SR microsomes. (C) Frequency of openings (Fo in events/min) of RyR2 channels in HC and DMD ± S107 SR microsomes. (D) Single channel Po in each DMD (1, 2 and 3) treated or not with S107. Data are presented as mean ± SEM. $^{**}P < 0.01$ (Mann–Whitney test). (E) Representative immunoblot bands of the three HC, three DMD and three DMD + S107 lysates under stress (1 μM of isoproterenol) for total RyR2, PKA-phosphorylated RyR2 at 2809 site (P2809), CaMKII-phosphorylated RyR2 at 2815 site (P2815), S-nitrosylation of cysteines (Cys-NO), RyR2 oxidation (DNP) and Castabin2 (FKBP12.6) binding. (F) Relative calstabin2 amount bound to RyR2 in HC hiPSC-CMs, DMD hiPSC-CMs and DMD hiPSC-CMs treated with S107. The number of experiments varies from three to nine in HC and DMD hiPSC-CM lysates. Data are presented as mean ± SEM. $^{**}P < 0.01$ (Kruskal–Wallis test).

To analyse the interactions between the identified com-mon targets, a protein–protein interaction (PPI) network was constructed using STRING. The PPI network obtained (P-value: 4.05e-8) consisted of 114 nodes (proteins). There were75 edges that indicated protein–protein associations both functional and/or physical, from the STRING pathway analysis the GO: Cellular component terms confirmed our previous results: extracellular matrix,

extracellular space and, collagen containing extracellular matrix (Figure S7A). Finally, we represented the differentially expressed proteins related to senescence and SASP in a heatmap (Figure S11B). Interestingly, dysregulated senescence-associated proteins in DMD hiPSC-CMs were normalized by S107 treatment (Figure S7B). We identified additional SASP factors that belong to the growth factor family, chemokine/cytokine family and ECM family that were induced in DMD hiPSC-CMs and downregulated by S107.

DMD hiPSC-CMs and GRMD hearts are characterized by premature cellular senescence

Dystrophin deficiency causes oxidative stress and genome in-stability, inducing premature senescence.18, 19 Based on these findings and proteomic profile, we hypothesized DMD hiPSC-CMs exhibit senescence. SA-βgal activity confirmed increased senescence in DMD hiPSC-CMs compared with HC hiPSC-CMs. S107 treatment significantly reduced SA-βgal-positive cells (Figure3A, B), indicating closed RyR2 prevents senescence. It has been shown that larger cell components, such as enlarged nucleoli, may be contributing to the larger overall sizes of senescent cells.20–22DMD hiPSC-CMs had larger nuclei than HC hiPSC-CMs (Figure3D), but S107 prevented nucleus enlargement (Figure3 E). All DMD groups exhibited reduced nucleus size under S107 treatment (Figure3F).

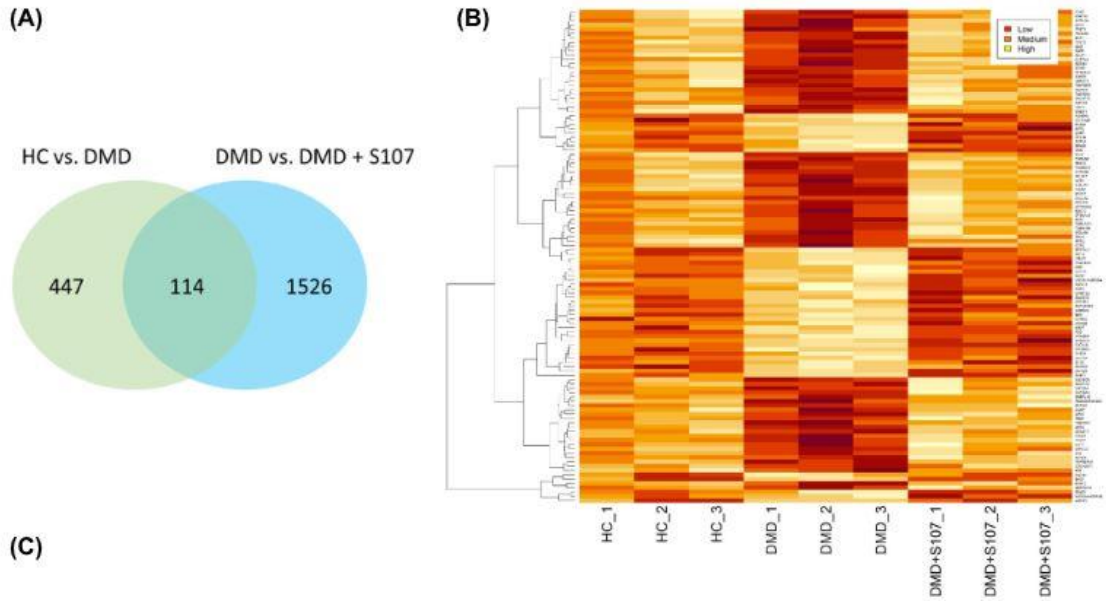

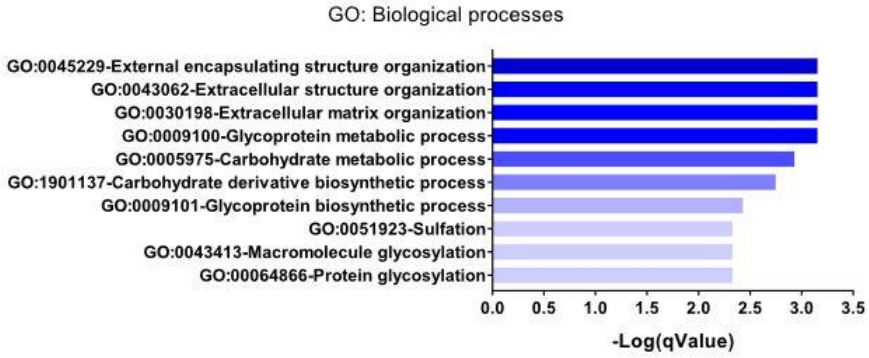

Figure 2 SR Ca^{2+} leak leads to signalling pathways involving fibrosis and senescence in DMD hiPSC-CMs. (A) Overlap of proteins above cut-off (*P*-value < 0.05 and |fold-change| ≥ 1.5) for HC versus DMD versus DMD + S107 comparisons. For S107 application, DMD hiPSC-CMs were treated with 5 μM S107 for 10 days in culture medium. (B) Heatmap of the differentially expressed proteins (DEPs) that are common to both HC versus DMD and DMD versus DMD treated with S107 comparisons. (C) Most representative dysregulated pathways in Gene Ontology analysis. The data are three biological replicates from the three HC and three DMD lines ± S107 treatment.

We performed qPCR to evaluate senescence markers p21, p15, and p16, as well as SASP components like TGFβ2, IL1α, IL1β, and IL6. DMD hiPSC-CMs showed higher p15 and p16 expression. S107 prevented p15 overexpression (Figure S8 B), while p21 and SASP components showed a tendency to increase in DMD hiPSC-CMs (Figure S8A–G).

To assess SASP proteins secreted by senescent DMD hiPSC-CMs, we performed a biotinylated Luminex assay for IL1α, IL1β, IL-6, IL18, IFNγ, and TNFα. IL1α, IL1β, and TNFα secretion remained unchanged (Figure S9A, B, F), while DMD hiPSC-CMs tended to secrete more IL6, IL18, and IFNγ (Figure S9C–E).S107 treatment appeared to prevent IL18 secretion (Figure S9D).

We hypothesized varying cardiac maturity in DMD hiPSC-CMs linked to cellular senescence. qPCR experiments for 13 cardiac markers showed lower RYR2 expression in DMD (Figure S10A). MYH6, MYH7, and MLC2 gene expression exhibited no significant difference (Figure S10B), but DMD hiPSC-CMs displayed a higher MYH7/MYH6ratio (Figure S10F). SR calcium handling proteins (CSQ, TRD, JUNCTIN, SERCA2A, PLB, and FKBP12.6) showed no change (Figure S10C, D). NCX and HCN4 gene expression were similar between HC and DMD hiPSC-CMs (Figure S10E).

To assess in vivo relevance, we used the cardiac GRMD animal model, examining biopsies at 6 and 12 months.12-month GRMD exhibited heart failure.5,1512-month GRMD showed a trend towards higher p21 expression compared with 6-month GRMD (P= 0.06) and 12-month WT cardiac biopsies (P= 0.11). Higher p16 and TGFß2 expression in12-month GRMD compared with 6-month GRMD and12-month WT (Figure4A–C), and increased IL6 in 12-monthGRMD compared with 6-month GRMD (Figure4D). No difference observed between WT and GRMD dogs for IL1βat any age (Figure4E).

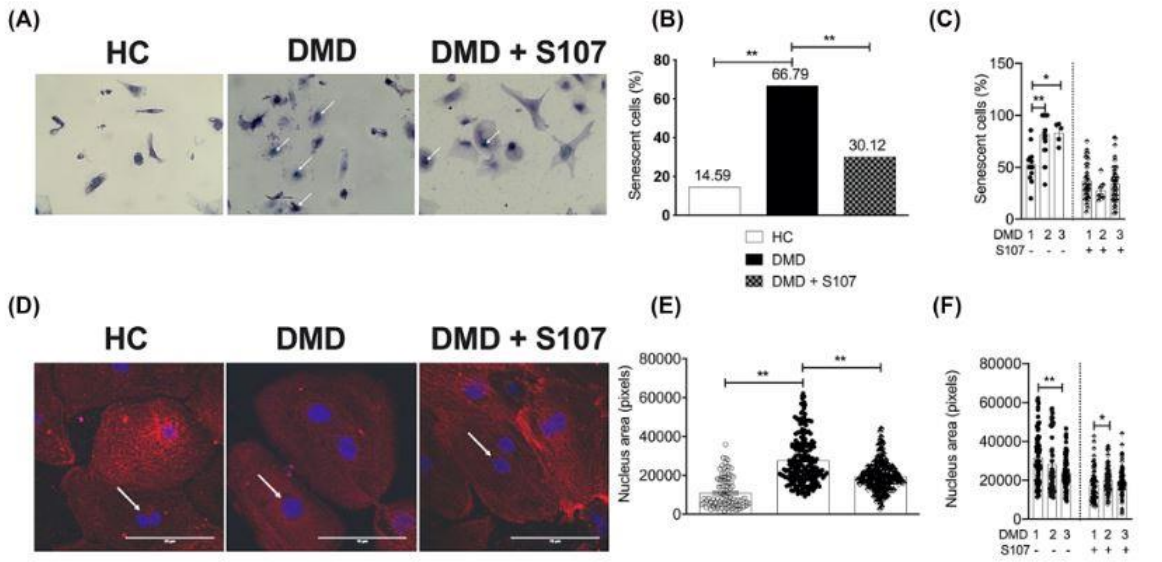

Figure 3 SR Ca^{2+} leak causes senescence in DMD hiPSC-CMs. (A) Representative images of HC hiPSC-CMs, DMD hiPSC-CMs and DMD hiPSC-CMs treated with S107 showing SA-β-gal blue staining (as represented by the white arrows). The acquisition was performed using EVOS XL Core imaging system microscopy (magnification ×40). For S107 application, DMD hiPSC-CMs were treated with 5 µM S107 for 10 days in culture medium. (B) Bar chart with each data point showing the percentage of SA-β-Gal-positive senescent cells in HC hiPSC-CMs (ratio of 47/322 cells, white bars), DMD hiPSC-CMs (ratio of 189/283 cells, black bars) and DMD hiPSC-CMs treated with S107 for 10 days (ratio of 432/1434 cells, grey bars). (C) Bar graphs summarizing the percentage of SA-β-gal-positive senescent cells in each DMD (1, 2 and 3) treated or not with S107 for 10 days. (D) Representative immunostaining for α actinin (in red) in HC hiPSC-CMs, DMD hiPSC-CMs and DMD hiPSC-CMs treated with S107 for 10 days. The nuclei are stained in blue (as represented by the white arrows). Scale bar: 10 µm. (E) Bar graphs summarizing the nucleus area (in pixels) in HC hiPSC-CMs, DMD hiPSC-CMs and DMD hiPSC-CMs treated with S107 for 10 days. (F) Nucleus area in each DMD (1, 2 and 3) treated or not with S107 for 10 days. The number of experiments varies from 99 to 240 for each graph. Data are represented as mean ± SEM. $*P < 0.05$, $**P < 0.01$ (Kruskal–Wallis test).

For comparison, we evaluated senescence in another cardiac disorder with diastolic Ca2+leak, using hiPSCs harbouring the RyR2-H29D mutation causing PMVT.9,12 No difference observed in senescence markers between PMVT hiPSC-CMs and isogenic controls (Figure S11A–G).

Fibrotic deposit and hypertrophy in DMD hiPSC-CMs

We hypothesized that extracellular matrix remodelling could be associated with fibrosis and morphological changes. Using lactate-based sorting to retain hiPSC-CMs in the dish, we assessed COL1A1 expression, a fibrosis marker, and found in-creased expression in DMD hiPSC-CMs (Figure5A, B). The three DMD groups showed varying fibrotic deposits, with higher levels in DMD 2. S107 treatment tended to reduce fibrosis in all three DMD groups, especially in DMD 3(Figure5 C). DMD hiPSC-CMs exhibited higher cell surface than HC hiPSC-CMs (Figure5A, D, E).

S107 treatment significantly reduced collagen1A (COL1A1)expression in DMD hiPSC-CMs (Figure5A, B) but did not pre-vent cellular hypertrophy (Figure5D). There were differences in cellular hypertrophy among the three DMD groups, all of which were abolished by S107 treatment (Figure5 E).

To understand the fibrotic components produced in DMD hiPSC-CMs, we examined vimentin (fibroblast marker), alpha smooth muscle actin (α-SMA, myofibroblast marker), and PDGF receptor α (PDGFRα) expression.23No PDGFRα signal was detected in HC and DMD hiPSC-CMs positive for the cardiac sarcomeric alpha-actinin marker (Figure S12A).

Interestingly, DMD hiPSC-CMs expressed higher levels ofα-SMA compared with HC hiPSC-CMs, while both HC and DMD TnI-positive hiPSC-CMs expressed vimentin (Figure S12B, C).

In-depth proteomic analysis revealed that pathways related to extracellular matrix (ECM) organization and integrin cell surface interactions were significantly altered in DMD hiPSC-CMs compared with HC hiPSC-CMs. Key ECM structural proteins, such as collagen1A, collagen3, ECM-1, and elastin, were upregulated in DMD hiPSC-CMs, and S107treatment prevented these changes. The log fold change (log2 FC) values for these proteins between DMD and HC hiPSC-CMs were 1.72, 1.77, 2.73, and 1.88, respectively. The 10-day S107 treatment of the three DMD hiPSC lines induced significant changes in syndecan proteins, integrin, and non-integrin cell surface interactions (Figure S12D and Tables S5 and S6).

S107prevents the aberrant intracellular Ca2+release in DMD hiPSC-CMs

Dystrophin deletion affects SR Ca2+handling in our three DMD patient-derived CMs. At rest, DMD hiPSC-CMs showed abnormal Ca2+handling with increased Ca2 + transients and diastolic leaky events (Figure S13A). DMD hiPSC-CMs exhibited higher Ca2+transient amplitude, dF/dt max, and decay time (Figure S13B, C, E) with increased frequency of diastolic leaky events (Figure S13D). Under stress, DMD hiPSC-CMs displayed aberrant Ca2+transients with increased diastolic leaky events (Figure6A). Diastolic Ca2+concentration was significantly higher in DMD hiPSC-CMs (Figure S14A). SR Ca2+content remained unchanged between HC and DMD hiPSC-CMs (Figure S14B–D).

S107 treatment on DMD hiPSC-CMs prevented abnormalCa2+release (Figure6A), leading to decreased dF/dt max, reduced frequency of diastolic leaky events, and shorter decay time (Figure 6C, D, E).

DMD hiPSC-CMs exhibit hypocontractility prevented by S107treatment

Duchenne DCM is characterized by hypocontractility.24,25 We assessed contractile properties of DMD hiPSC-CMs in 2Dsheets and observed impaired contraction/relaxation cycles compared with HC hiPSC-CMs (Figure S15A). Beat rate showed no significant difference (Figure S15B) but DMD hiPSC-CMs had lower average amplitude (Figure S15C) and increased contraction and relaxation time (Figure S15D,E).Resting time showed no significant difference (Figure S15F).Isoproterenol application perturbed contraction/relaxation cycles in DMD hiPSC-CMs but remained stable in HC hiPSC-CMs (Figure7A). Beat rate was higher in DMD hiPSC-CMs (Figure7B), and they had lower average amplitude (Figure7C) and decreased resting time (Figure7F) compared with HC. The differentiating factor, representing contractile differences, significantly changed between HC and DMD hiPSC-CMs (Figure S16A). S107 treatment decreased beat rate (Figure7B) and increased average amplitude and resting time (Figure7C,F). DMD + S107 hiPSC-CMs showed a higher differentiating factor, similar to HC (Figure S16A). Sarcomere length in DMD hiPSC-CMs was shorter than HC, but S107 re-stored it (Figure S17A,B).

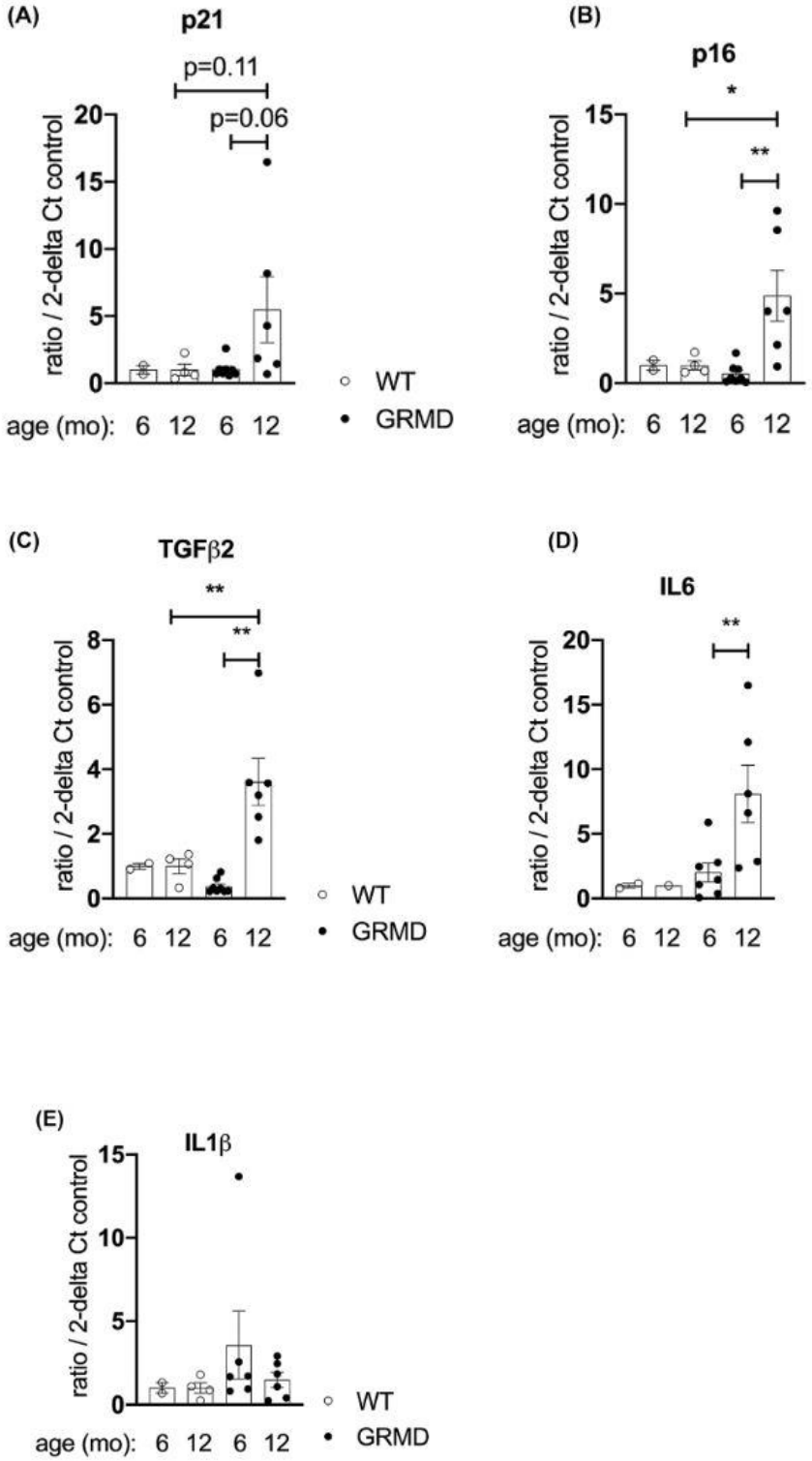

Figure 4 GRMD aged of 12 months exhibit senescence. Bar graphs summarizing the fold change in gene expression analysis for p21 (cyclin-dependent kinase inhibitor 1) (A), p16 (cyclin-dependent kinase inhibitor 2A) (B), TGFβ2 (transforming growth factor-beta 2) (C) IL6 (interleukin 6) (D) and IL1β (interleukin 1 beta) (E) in WT (white dot plots) and GRMD (black dot plots) cardiac biopsies at 6- and 12-month-old. Data are represented as mean ± SEM. $*P < 0.05$, $**P < 0.01$ (Kruskal–Wallis test).

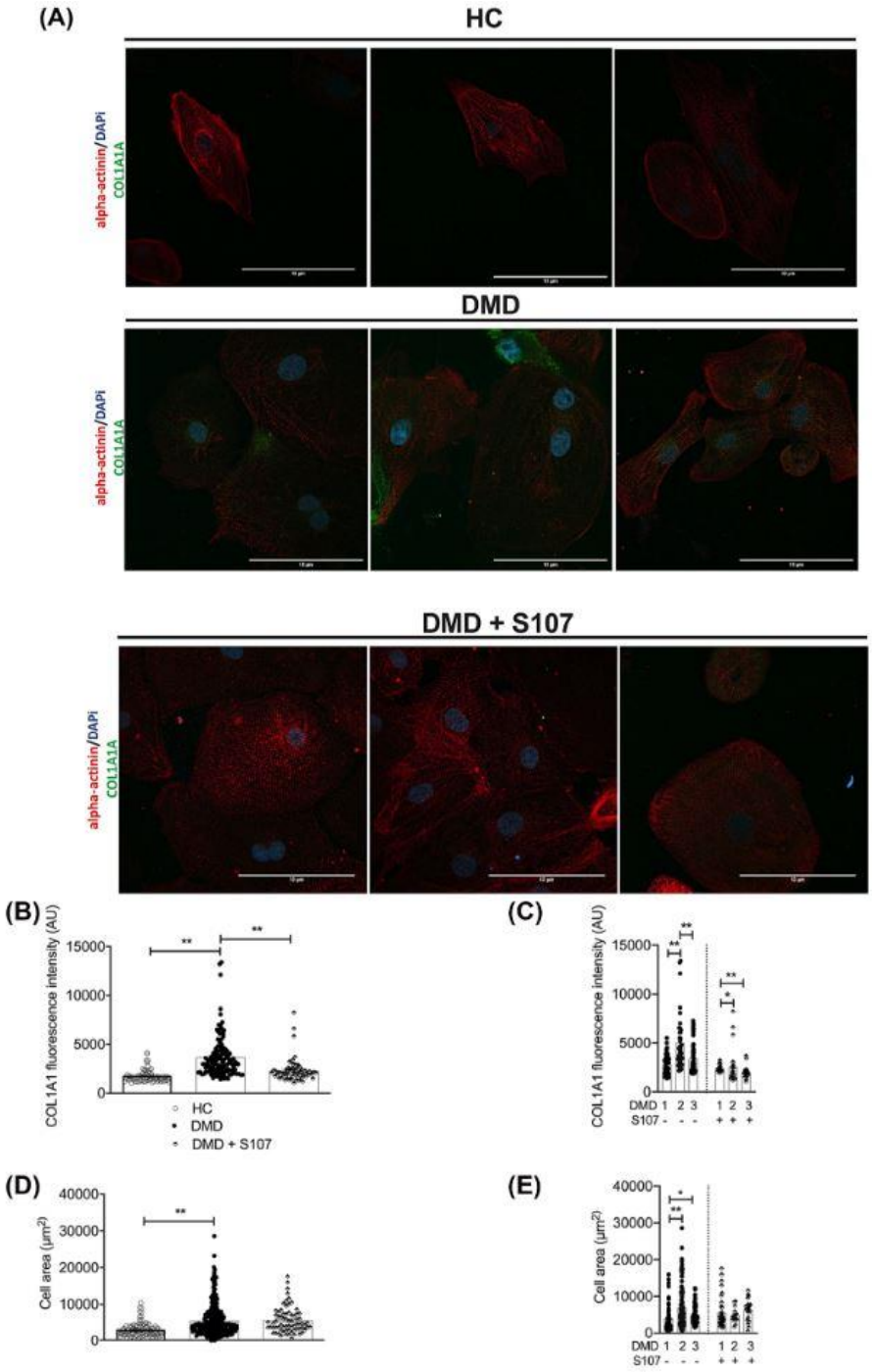

Figure 5 S107 prevents the fibrotic deposit in hypertrophic DMD hiPSC-CMs. (A) Immunostaining for α actinin (in red) and collagen type 1 α 1 (COL1A1) (in green) in HC hiPSC-CMs, DMD hiPSC-CMs and DMD hiPSC-CMs treated with S107. The nuclei are stained in blue. For S107 application, DMD hiPSC-CMs were treated with 5 µM S107 for 10 days in culture medium. Scale bar: 10 µm. (B) COL1A1 fluorescence intensity (AU) in HC hiPSC-CMs (white dot plots), DMD hiPSC-CMs (black dot plots) and DMD hiPSC-CMs treated with S107 (diamond plots). The number of experiments varies from 66 to 134 for each graph. (C) COL1A1 fluorescence intensity (AU) in each DMD (1, 2 and 3) treated or not with S107. (D) Cell area (μm^2) in HC hiPSC-CMs, DMD hiPSC-CMs and DMD hiPSC-CMs treated with S107. (E) Cell area in each DMD (1, 2 and 3) treated or not with S107. The number of experiments varies from 71 to 242 for each graph. Data are represented as mean ± SEM, $^{**}P < 0.01$ (Kruskal–Wallis test).

Discussion

In this study, we employed patient-specific DMD hiPSC-CMs to reveal cellular defects associated with SR Ca2+leak viaRyR2. We have demonstrated that aberrant SR Ca2+handlingis an early pathophysiological feature in DMD mouse (mdx), DMD canine (GRMD) and human CMs.3–5While the three DMD patients exhibit normal LVEF and early defects by STE at the time of the blood sample taking, our findings revealed that SR Ca2+leak and RyR2 post-translational remodelling are common and early-stage pathological features in DMD hiPSC-CMs and trigger dramatic cardiac consequences including cardiac hypertrophy and fibrosis, hypocontractility, sarco-mere disorganization and senescence. Preventing RyR2 dysfunction with S107 improves the intracellular Ca2+dynamicsand restores normal contractility and prevents fibrosis development and senescence.

We showed that RyR2 channels are directly involved in the SR Ca2+leak in patient-specific DMD hiPSC-CMs. Ca2+leakfrom RyR2 was observed in the three DMD patient lines with no difference between them. These results suggest a com-mon pathological signature in DMD, although the dystrophin mutations are different (DMD 1, 2 and 3, harbouring exon 1,52 and 55 deletions, respectively) with a very early RyR2 dysfunction. These results suggest that RyR2 dysfunction is a very proximal mechanism in DMD.

Stabilizing RyR2 channels prevents the abnormal RyR2 leak in the three DMD patient lines. We found PKA-hyper-phosphorylated RyR2 depleted of calstabin2 at rest, suggesting that DMD hiPSC-CMs have increased basal level of PKA-phosphorylation and S-nitrosylated and oxidized. It has been reported that NO production by eNOS can increase Ca2+spontaneous sparks with a direct S-nitrosylation of RyR2.26These results agree with our RyR2 data under resting conditions. It is also possible that increased activity of iNOS could lead to RyR2 hyper-S-nitrosylation. Under stress conditions, RyR2 channels were only calstabin2 depleted. These results differ from those we have obtained inmdxmice.4 They also supported the blunted ß-adrenergic receptor response in DMD hiPSC-CMs.3,27The significance of such differences be-tween human and mouse RyR2 remodelling are unclear and require further experiments. One can however suspect that other components in vivo such as the autonomic nervous sys-tem, may also account.

We confirmed that the intracellular Ca2+handling is perturbed in DMD hiPSC-CMs derived from three DMD patients. They confirm our results on two other DMD hiPSClines.3It supports that the dystrophin deficiency causes a com-mon pathological signature in murine, dog and humanmodels.4,5

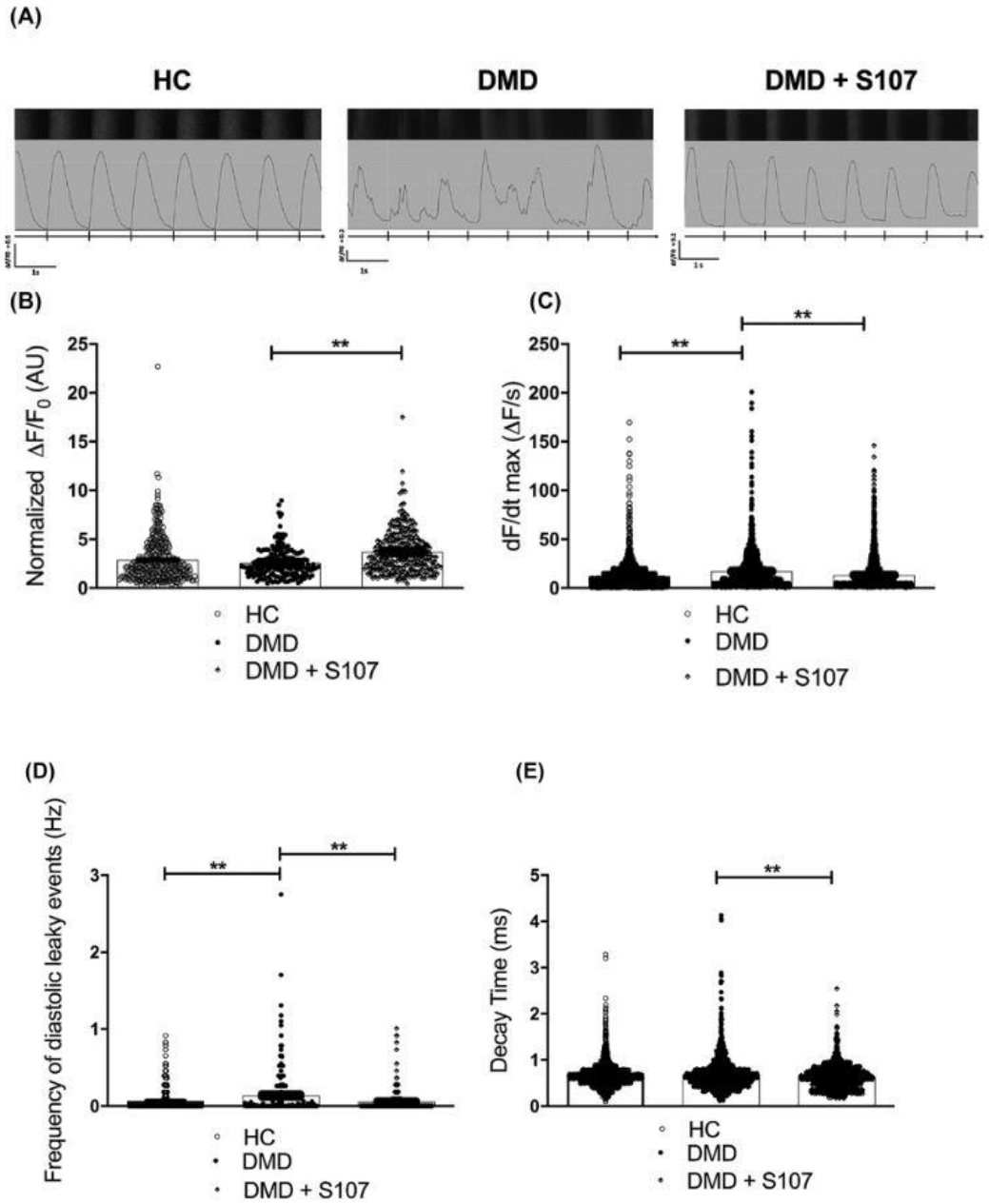

Figure 6 S107 prevents the stress-induced aberrant release of Ca^{2+} in DMD hiPSC-CMs. (A) Representative original line-scan of Ca^{2+} and corresponding Ca^{2+} transients in HC, DMD hiPSC-CMs and DMD hiPSC-CMs treated with S107 (5 μM overnight) under stress conditions (1 μM isoproterenol and 1 Hz pacing at 20 V for 5 ms duration). (B) Normalized Ca^{2+} amplitude (AU) in HC hiPSC-CMs (white dot plots), DMD hiPSC-CMs (black dot plots) and DMD hiPSC-CMs treated with S107 (diamond plots). (C) Rate of RyR2 Ca^{2+} release (dF/dtmax in ΔF/s) in HC hiPSC-CMs, DMD hiPSC-CMs and DMD hiPSC-CMs treated with S107. (D) Frequency of diastolic leaky events (Hz) in HC hiPSC-CMs, DMD hiPSC-CMs and DMD hiPSC-CMs treated with S107. (E) Decay time (ms) in HC hiPSC-CMs, DMD hiPSC-CMs and DMD hiPSC-CMs treated with S107. The number of experiments varies from 178 to 370 cells for each graph. Data are represented as mean ± SEM. $^{**}P < 0.01$ (Kruskal–Wallis test).

Our clinical results showed that the three DMD patients have normal LVEF but early defects by STE at the time of the blood sample. The DMD 3 exhibited LV segmental longitudinal strain decrease at the 2 time points. We and others have reported such pathological feature of DMD-associated DCM using hiPSC-CMs.3,24,25,28More recently, we showed left ventricular dysfunction in mdx mice and GRMD dogs, a defect that is prevented by specifically stabilizing RyR2.5Here, we found that DMD hiPSC-CMs display aberrant contraction cycles accompanied by lower amplitude which may reflect hypocontractility. This was associated with disorganized sarcomeres, short in length. It has been shown that GRMD

and mdx models also exhibit altered myofilament structure and sarcomere remodelling.5,29,30Interestingly, stabilizing RyR2 with S107 prevents both the hypocontractility and sarcomere length remodelling in DMD hiPSC-CMs and restores the contractile/relaxation properties similar to those in HC hiPSC-CMs, and in full agreement with our re-cent observations on GRMD dogs treated with RyR2stabilizer.5Upon stress, DMD hiPSC-CMs exhibit higher beating rate which indicates tachycardia consistently with the clinical report that DMD patients have a significantly higher rate of ventricular tachycardia.31Higher beat rate in DMD hiPSC-CMs was reversed by S107. These results, in addition to our previous ones on animal models, 4, 5 support that targeting the SR Ca2+machinery, in particular RyR2, rescued hypocontractility in DMD.

We here demonstrated, in line with leaky RyR2, DMD hiPSC-CMs exhibit a profile of premature senescence, with higher gene and protein expression of the senescence markers SA-βgal, p15/p16, nuclear enlargement and cell hypertrophy. The premature senescence was not found in a model of inherited cardiopathy (i.e., PMVT) in which RyR2 is mutated and causes SR Ca2+leak.9,12 These results indicate that another gene mutation does not cause senescence al-though it leads to SR Ca2+leak. Differences in RyR2 properties and SR Ca2+leak intensity may explain why dystrophin deficiency causes senescence compared with PMVT. We found that DMD hiPSC-CMs have less RyR2 expressed and a different ratio of MYH7/MYH6 suggesting a different maturity degree. Considering the treatment with Pluricyte medium containing T3,32Yanget al. have shown that T3 further improves the maturity of hiPSC-CMs but favours MYH6 overMYH7 expression.33Our data suggest that dystrophin deficiency causes a further mature ventricular-like phenotype with higher MYH7/MYH6 ratio and senescence upon T3 treatment. Senescence was confirmed in the canine DMD (GRMD) model, proving its specificity in Duchenne DCM. Interestingly, the three DMD patient lines exhibited senescence independently of the dystrophin mutation they harboured. Our results revealed the senescence as a novel common pathological feature in DMD patient-derived CMs, which is associated with SR Ca2+leak. Using DMD hiPSC-CMs, a recent study revealed progressive and mechanosensitive telomere shortening associated with contractile dysfunction.34In the present study, using GRMD cardiac biopsies of 6- and 12-month, we observed that GRMD dogs of 12-month, specifically selected for heart failure, 5, 15 exhibit increased expression of senescent markers including p21, p16, TGFß2 and IL6. Notably, our observations revealed intriguing trends in GRMD dogs with heart failure, wherein they displayed a higher level of senescence compared with age-matched WT dogs, albeit with some variability. Strikingly, the senescence levels in these heart failure-affected GRMD dogs were even higher than in GRMD dogs aged 6 months, suggesting a potential link be-tween dilated cardiomyopathy (DCM), heart failure, and senescence in the context of Duchenne muscular dystrophy (DMD). Importantly, the senescence observed in GRMD dogs appears to be associated with RyR2 Ca2+leak, further supporting the notion that RyR2 dysfunction may play a role in the senescence process.5

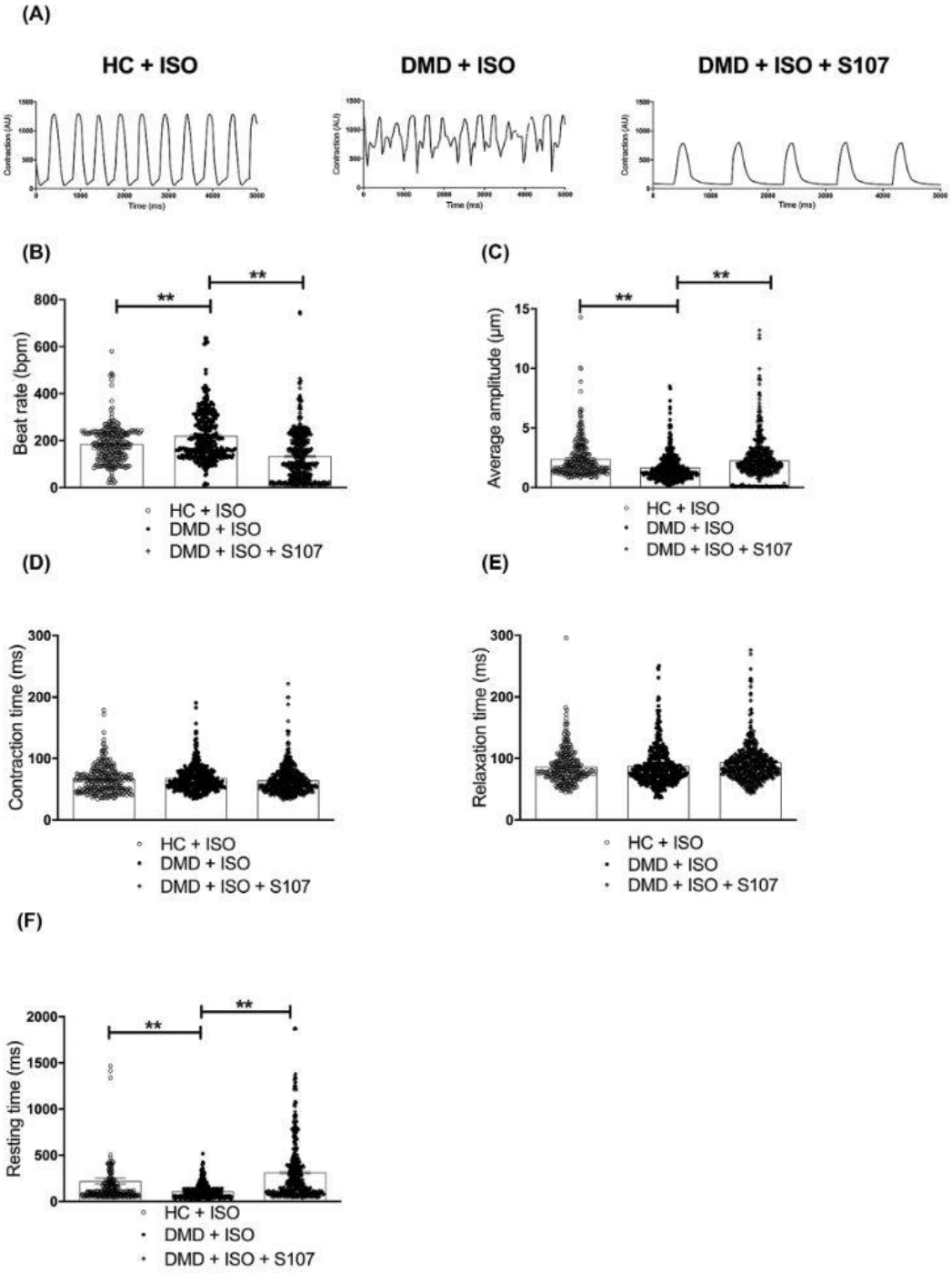

Figure 7 S107 prevents the stress-induced hypocontractility in DMD hiPSC-CMs. (A) Representative traces of video-edge capture recordings in HC hiPSC-CMs, DMD hiPSC-CMs ± S107 (5 µM overnight) in presence of 1 µM isoproterenol (ISO). (B) Beat rate (bpm) in HC hiPSC-CMs (white dot plots), DMD hiPSC-CMs (black dot plots) and DMD hiPSC-CMs + S107 (diamond plots). (C) Average amplitude (µm) in HC hiPSC-CMs, DMD hiPSC-CMs and DMD hiPSC-CMs + S107. (D) Contraction time (ms) in HC hiPSC-CMs, DMD hiPSC-CMs and DMD hiPSC-CMs treated with S107. (E) Relaxation time (ms) in HC hiPSC-CMs, DMD hiPSC-CMs and DMD hiPSC-CMs + S107. (F) Resting time (ms) in HC hiPSC-CMs, DMD hiPSC-CMs and DMD hiPSC-CMs + S107. The number of experiments varies from 130 to 630 for each dot plot. Data are represented as mean ± SEM. $**P < 0.01$ (Kruskal–Wallis test).

It was recently shown that oxidative stress and telomere damage were the main drivers of post-mitotic senescence in cardiomyocytes. Senescent cell ablation decreased hypertrophy and fibrosis in the aging heart.35 Telomere dysfunction and oxidative stress have also been demonstrated to be involved in heart failure in DMD, as long telomeres could protect mdx mice from dystrophic cardiomyopathy.36,37Here,we provide new findings indicating that

DMD cardiomyopathy is characterized by the induction of premature senescence, revealed by higher SA-βgal activity, increase in cell size and nuclear size and increased mRNA expression of senescence markers.38 Preventing RyR2 Ca2+leak using S107 was able to reduce senescence markers (SA-βgal, nuclear size,p15) in DMD hiPSC-CMs. S107 treatment for 10 days rather than overnight was aimed at potentially targeting deeper molecular mechanisms involved in senescence. The senescence that we observed in DMD hiPSC-CMs and that we confirmed in GRMD cardiac biopsies could have further impact on the cardiac microenvironment through the secretion of a SASP. Our proteomic analysis confirmed these findings with further expressed proteins related to SASP in DMD. This phenotype was prevented by S107 treatment, supporting the link be-tween RyR2 Ca2+leak and senescence. We observed an in-crease in pro-inflammatory cytokines in the extracellular media of DMD hiPSC-CMs. Some of them increased significantly, for the others a tendency was observed. Nevertheless, they could have additive effects if together secreted. Importantly, the SASP is known to mediate deleterious effects in such as paracrine senescence, inflammation and fibrosis, which are detrimental features of DMD cardiomyopathy. In agreement with our results, the deleterious impact of senescent cells has recently been established in muscular dystrophy progression in DMD rats, indicating that senescence might be a general mechanism in both DMD heart and skeletal muscles.39 Dilated cardiomyopathy is characterized by myocyte hyper-trophy andfibrosis.40Our study on DMD hiPSC-CMs also revealed higher cell surface, indicating cell hypertrophy, consistent with previousfindings.40The hypertrophic characteristics of DMD hiPSC-CMs were observed after 30 days of maturation using Pluricyte medium, which enhances the morphological and functional features of hiPSC-CMs.32 How-ever, another study by Eguchi et al. found smaller-sized DMD hiPSC-CMs at 30 days of differentiation, suggesting that the maturity state of the cells may influence their size.41 Stabilizing RyR2 using S107 did not prevent cell hypertrophy in our experimental conditions, indicating the need for further investigation into the mechanism. The 10-day S107 treatment of DMD hiPSC-CMs led to changes in syndecan proteins, integrin, and non-integrin cell surface interactions, known to be involved in fibrosis and cardiac hypertrophy. These structural changes may be a compensatory response to altered contractile properties, as suggested by previous studies.40 We found that DMD hiPSC-CMs exhibited fibrosis, consistent with findings in mdx mice and age-dependent fibrosis in DMD hiPSC-CMs.42 Our data indicate that DMD hiPSC-CMs themselves produce COL1A1 and expressαSMA, contributing to interstitial fibrosis at an early stage. Interestingly, both HC and DMD hiPSC-CMs expressed vimentin filaments, a feature typically present in human fetal hearts but not in adults.43 This suggests that under certain pathological conditions, cardiomyocytes may undergo changes leading to the production of ECM components and alterations in their sarcomeric structure. Proteomic analysis confirmed significant change sin extracellular matrix organization and structure in DMD hiPSC-CMs, which were prevented by S107, further supporting the link between fibrosis and Ca2+leak. Myocardial fibrosis is one of the earliest clinical features in the diagnosis of dystrophic cardiac pathology, and our findings in DMD hiPSC-CMs recapitulate this clinical situation. In addition to cardiomyocytes, other cell types might contribute to fibrosis in culture. However, fibroblasts and myofibroblasts lack ryanodine receptor expression and are unresponsive to caffeine, which activates RyR1 and

RyR2.44 As S107 selectively targets RyR1 and RyR2, our data strongly indicate that fibroblasts and myofibroblasts are not directly involved in preventing S107-induced fibrosis.

These data suggest that cellular damages occur earlier than cardiac clinical pathology in DMD patients, with significant perturbation of cardiac ECC. RyR2 emerges as an early bio-marker for DMD-associated cardiac damages. Early-stage cardiac alterations were indicated by STE analysis in DMD boys, mice, and GRMD, and these changes could be linked to the observed premature fibrosis and hypocontractility in DMD hiPSC-CMs.5The progressive onset of DCM may be associated with increased fibrosis and premature senescence, leading to cell death and further cardiac fibrosis in a vicious cycle, resulting in hypocontractility as a major feature of DCM. We understand the importance of isogenic controls in genetic studies for minimizing genetic variability and strengthening causal relation-ships between mutations and phenotypes. Despite this aware-ness, we recognize the limitations in our study due to the absence of isogenic controls and potential influences of broader genetic factors beyond DMD mutations. Our primary goal is to investigate the early pathological signature of a com-mon RyR2 dysfunction in DMD regardless of the mutation. We acknowledge that our approach provides valuable insights but represents only one aspect of this complex disease, not ac-counting for its full genetic variability.

In conclusion, our study highlights the potential of hiPSC-CMs as a valuable tool to understand the molecular mechanisms underlying early-stage dystrophin deficiency and the development of Duchenne DCM.

Conflict of interest

A.R.M. is a board member and owns shares in ARMGO Pharma Inc., which is targeting RyR channels for therapeutic purposes. The rest of the authors declare no conflict of interest.

Acknowledgements

We acknowledge the imaging facility MRI, member of the national infrastructure France-BioImaging infrastructure sup-ported by the French National Research Agency (ANR-10-INBS-04, «Investments for the future»).Funding This work was supported by grants of the French Muscular Dystrophy Association (AFM; projects 15083, 16073, MNM22012, 20225, 14389, 15208, 15632, 16396 and 17124), the ‘Fondation de la Recherche Médicale’(FRM; SPF20130526710), the ‘Institut National pour la Santé et la Recherche Médicale’(INSERM), and the ‘Fondation Coeur et Recherche’. Yvonne Sleiman received a postdoctoral fellowship from ‘Le Fonds Marion Elisabeth Brancher’.

References

1. Kamdar F, Garry DJ. Dystrophin-deficient cardiomyopathy. J Am Coll Cardiol 2016;67:2533-2546.
2. Connuck DM, Sleeper LA, Colan SD, Cox GF, Towbin JA, Lowe AM, et al. Characteristics and outcomes of cardiomyopathy in children with Duchenne or Becker muscular dystrophy: a comparative study from the Pediatric Cardiomyopathy Registry. Am Heart J 2008;155:998-1005.
3. Jelinkova S, Vilotic A, Pribyl J, Aimond F, Salykin A, Acimovic I, et al. DMD pluripotent stem cell derived cardiac cells recapitulate in vitro human cardiac pathophysiology. Front Bioeng Biotechnol 2020;8:535.
4. Fauconnier J, Thireau J, Reiken S, Cassan C, Richard S, Matecki S, et al. Leaky RyR2 trigger ventricular arrhythmias in Duchenne muscular dystrophy. Proc Natl Acad Sci U S A 2010;107:1559-1564.
5. Cazorla O, Barthélémy I, Su JB, Meli AC, Chetboul V, Scheuermann V, et al. Stabilizing ryanodine receptors improves left ventricular function in juvenile dogs with Duchenne muscular dystrophy. J Am Coll Cardiol 2021;78:2439-2453.
6. Moreau A, Reisqs J-B, Delanoe-Ayari H, Pierre M, Janin A, Deliniere A, et al. Deciphering DSC2 arrhythmogenic cardiomyopathy electrical instability: from ion channels to ECG and tailored drug therapy. Clin Transl Med 2021;11:e319.
7. Souidi M, Amédro P, Meyer P, Desprat R, Lemaître J-M, Rivier F, et al. Generation of three Duchenne muscular dystrophy patient-specific induced pluripotent stem cell lines DMD_YoTaz_PhyMedEXp, DMD_RaPer_PhyMedEXp, DMD_OuMen_PhyMedEXp (INSRMi008-A, INSRMi009-A and INSRMi010-A). Stem Cell Res 2020;49:102094.
8. Souidi M, Sleiman Y, Acimovic I, Pribyl J, Charrabi A, Baecker V, et al. Oxygen is an ambivalent factor for the differentiation of human pluripotent stem cells in cardiac 2D monolayer and 3D cardiac spheroids. Int J Mol Sci 2021;22:662.
9. Sleiman Y, Souidi M, Kumar R, Yang E, Jaffré F, Zhou T, et al. Modeling polymorphic ventricular tachycardia at rest using patient-specific induced pluripotent stem cell-derived cardiomyocytes. EBioMedicine 2020;60:103024.
10. Acimovic I, Refaat MM, Moreau A, Salykin A, Reiken S, Sleiman Y, et al. Post-translational modifications and diastolic calcium leak associated to the novel RyR2-D3638A mutation lead to CPVT in patient-specific hiPSC-derived cardiomyocytes. J Clin Med 2018;7:423.
11. Fauconnier J, Meli AC, Thireau J, Roberge S, Shan J, Sassi Y, et al. Ryanodine receptor leak mediated by caspase-8 activation leads to left ventricular injury after myocardial ischemia-reperfusion. Proc Natl Acad Sci U S A 2011;108:13258-13263.
12. Cheung JW, Meli AC, Xie W, Mittal S, Reiken S, Wronska A, et al. Short-coupled polymorphic ventricular tachycardia at rest linked to a novel ryanodine receptor (RyR2) mutation: leaky RyR2 channels under non-stress conditions. Int J Cardiol 2015;180:228-236.
13. Jozwiak M, Meli AC, Melka J, Rienzo M, d'Anglemont de Tassigny A, Saint N, et al. Concomitant systolic and diastolic alterations during chronic hypertension in pig. J Mol Cell Cardiol 2019;131:155-163.
14. Meli AC, Refaat MM, Dura M, Reiken S, Wronska A, Wojciak J, et al. A novel ryanodine receptor mutation linked to sudden death increases sensitivity to cytosolic calcium. Circ Res 2011;109:281-290.

15. Su JB, Cazorla O, Blot S, Blanchard-Gutton N, Ait Mou Y, Barthélémy I, et al. Bradykinin restores left ventricular function, sarcomeric protein phosphorylation, and e/nNOS levels in dogs with Duchenne muscular dystrophy cardiomyopathy. Cardiovasc Res 2012;95:86-96.
16. Zanou N, Dridi H, Reiken S, Imamura de Lima T, Donnelly C, de Marchi U, et al. Acute RyR1 Ca(2+) leak enhances NADH-linked mitochondrial respiratory capacity. Nat Commun 2021;12:7219.
17. Wang Q, Wang W, Wang G, Rodney GG, Wehrens XHT. Crosstalk between RyR2 oxidation and phosphorylation contributes to cardiac dysfunction in mice with Duchenne muscular dystrophy. J Mol Cell Cardiol 2015;89:177-184.
18. Jelinkova S, Fojtik P, Kohutova A, Vilotic A, Marková L, Pesl M, et al. Dystrophin deficiency leads to genomic instability in human pluripotent stem cells via NO synthase-induced oxidative stress. Cell 2019;8:53.
19. da Silva PFL, Schumacher B. DNA damage responses in ageing. Open Biol 2019;9:190168.
20. Buchwalter A, Hetzer MW. Nucleolar expansion and elevated protein translation in premature aging. Nat Commun 2017;8:328.
21. Tiku V, Jain C, Raz Y, Nakamura S, Heestand B, Liu W, et al. Small nucleoli are a cellular hallmark of longevity. Nat Commun 2017;8:16083.
22. Wang M, Lemos B. Ribosomal DNA harbors an evolutionarily conserved clock of biological aging. Genome Res 2019;29:325-333.
23. Ivey MJ, Kuwabara JT, Riggsbee KL, Tallquist MD. Platelet-derived growth factor receptor-α is essential for cardiac fibroblast survival. Am J Physiol-Heart Circulatory Physiol 2019;317:H330-H344.
24. Bollen IAE, van der Meulen M, de Goede K, Kuster DWD, Dalinghaus M, van der Velden J. Cardiomyocyte hypocontractility and reduced myofibril density in end-stage pediatric cardiomyopathy. Front Physiol 2017;8:1103.
25. Movsesian MA, Bristow MR. Alterations in cAMP-mediated signaling and their role in the pathophysiology of dilated cardiomyopathy. Academic Press; 2005. p 25-48.
26. Petroff MGV, Kim SH, Pepe S, Dessy C, Marbán E, Balligand J-L, et al. Endogenous nitric oxide mechanisms mediate the stretch dependence of Ca2+ release in cardiomyocytes. Nat Cell Biol 2001;3:867-873.
27. Mekies LN, Regev D, Eisen B, Fernandez-Gracia J, Baskin P, Ben Jehuda R, et al. Depressed β-adrenergic inotropic responsiveness and intracellular calcium handling abnormalities in Duchenne muscular dystrophy patients' induced pluripotent stem cell-derived cardiomyocytes. J Cell Mol Med 2021;25:3922-3934.
28. Atmanli A, Chai AC, Cui M, Wang Z, Nishiyama T, Bassel-Duby R, et al. Cardiac myoediting attenuates cardiac abnormalities in human and mouse models of Duchenne muscular dystrophy. Circ Res 2021;129:602-616.
29. Ait Mou Y, Lacampagne A, Irving T, Scheuermann V, Blot S, Ghaleb B, et al. Altered myofilament structure and function in dogs with Duchenne muscular dystrophy cardiomyopathy. J Mol Cell Cardiol 2018;114:345-353.
30. Varga B, Meli AC, Radoslavova S, Panel M, Lacampagne A, Gergely C, et al. Internal structure and remodeling in dystrophin-deficient cardiomyocytes using second harmonic generation. Nanomed Nanotechnol Biol Med 2020;30:102295.
31. Amedro P, Vincenti M, De La Villeon G, Lavastre K, Barrea C, Guillaumont S, et al. Speckle-tracking echocardiography in children with Duchenne muscular dystrophy: a

prospective multicenter controlled cross-sectional study. J Am Soc Echocardiogr 2019;32:412-422.
32. Ribeiro MC, Tertoolen LG, Guadix JA, Bellin M, Kosmidis G, D'Aniello C, et al. Functional maturation of human pluripotent stem cell derived cardiomyocytes in vitro - correlation between contraction force and electrophysiology. Biomaterials 2015;51:138-150.
33. Yang X, Rodriguez M, Pabon L, Fischer KA, Reinecke H, Regnier M, et al. Tri-iodo-L-thyronine promotes the maturation of human cardiomyocytes-derived from induced pluripotent stem cells. J Mol Cell Cardiol 2014;72:296-304.
34. Chang ACY, Pardon G, Chang ACH, Wu H, Ong SG, Eguchi A, et al. Increased tissue stiffness triggers contractile dysfunction and telomere shortening in dystrophic cardiomyocytes. Stem Cell Reports 2021;16:2169-2181.
35. Anderson R, Lagnado A, Maggiorani D, Walaszczyk A, Dookun E, Chapman J, et al. Length-independent telomere damage drives post-mitotic cardiomyocyte senescence. EMBO J 2019;38:e100492.
36. Chang ACY, Ong S-G, LaGory EL, Kraft PE, Giaccia AJ, Wu JC, et al. Telomere shortening and metabolic compromise underlie dystrophic cardiomyopathy. Proc Natl Acad Sci 2016;113:13120-13125.
37. Lee H-W, Blasco MA, Gottlieb GJ, Horner JW, Greider CW, DePinho RA. Essential role of mouse telomerase in highly proliferative organs. Nature 1998;392:569-574.
38. Manzella N, Santin Y, Maggiorani D, Martini H, Douin-Echinard V, Passos JF, et al. Monoamine oxidase-A is a novel driver of stress-induced premature senescence through inhibition of parkin-mediated mitophagy. Aging Cell 2018;17:e12811.
39. Sugihara H, Teramoto N, Nakamura K, Shiga T, Shirakawa T, Matsuo M, et al. Cellular senescence-mediated exacerbation of Duchenne muscular dystrophy. Sci Rep 2020;10:16385.
40. Pioner JM, Guan X, Klaiman JM, Racca AW, Pabon L, Muskheli V, et al. Absence of full-length dystrophin impairs normal maturation and contraction of cardiomyocytes derived from human-induced pluripotent stem cells. Cardiovasc Res 2020;116:368-382.
41. Eguchi A, Gonzalez AFGS, Torres-Bigio SI, Koleckar K, Birnbaum F, Zhang JZ, et al. TRF2 rescues telomere attrition and prolongs cell survival in Duchenne muscular dystrophy cardiomyocytes derived from human iPSCs. Proc Natl Acad Sci 2023;120:e2209967120.
42. Farini A, Gowran A, Bella P, Sitzia C, Scopece A, Castiglioni E, et al. Fibrosis rescue improves cardiac function in dystrophin-deficient mice and Duchenne patient-specific cardiomyocytes by immunoproteasome modulation. Am J Pathol 2019;189:339-353.
43. Kim H-D. Expression of intermediate filament desmin and vimentin in the human fetal heart. Anat Rec 1996;246:271-278.
44. Chen J-B, Tao R, Sun H-Y, Tse H-F, Lau C-P, Li G-R. Multiple Ca2+ signaling pathways regulate intracellular Ca2+ activity in human cardiac fibroblasts. J Cell Physiol 2010;223:68-75.